Removal of copper ions from aqueous solutions by kaolinite and batch design

Mahir Alkan, Burcu Kalay, Mehmet Doğan *, Özkan Demirbaş

Balikesir University, Faculty of Science and Literature, Department of Chemistry, 10145 Cagis-Balikesir, Turkey

Abstract

The removal of copper ions from aqueous solutions by kaolinite was investigated by using a batch-type method. Effects of factors such as pH, ionic strength, temperature, acid-activation and calcination on copper adsorption were investigated. The uptake of copper was determined from changes in concentration as measured by atomic absorption spectrometry. The extent of copper adsorption increased with increasing pH and temperature and with decreasing ionic strength, acid-activation and calcination temperature. The Langmuir and Freundlich adsorption models were used to determine the isotherm parameters associated with the adsorption process. The results provide support for the adsorption of copper ions onto kaolinite. Thermodynamic parameters indicated the endothermic nature of copper adsorption on kaolinite. The experimental results were applied a batch design. As a result, the kaolinite may be used for removal of copper ions from aqueous solutions.
© 2007 Elsevier B.V. All rights reserved.

Keywords: Kaolinite; Copper ion; Adsorption

1. Introduction

The removal of toxic heavy-metal contaminants from industrial waste waters is one of the most important environmental issues to be solved today. The major increase in the use of heavy metals has resulted in an increased concentration of metals in aquatic systems. There are numerous sources of industrial effluents leading to heavy metal discharges apart from the mining and metal related industries [1–3]. Because of their toxicity and non-biodegradable nature, metals are of special significance. The presence of heavy metals in wastewater and surface water is becoming a severe environmental and public health problem. A number of technologies have been developed to remove toxic copper from water. The most important technologies of these includes chemical precipitation, ion exchange, reverse osmosis and adsorption. But due to high maintenance cost these methods do not suit the needs of developing countries [4]. Chemical precipitation has been traditionally proposed to remove heavy metals from aqueous solutions. However, metal removal in the precipitation-coagulation systems is, in many cases, insufficient to meet strict regulatory requirements. Adsorption has been shown to be an economically feasible alternative method for removing trace metals from water. Heavy metals can be removed by adsorption on solid matrices. Adsorption process modelling is nowadays a topic of interest for the prediction of the metal partitioning between the aqueous solution and the solid surface, and its subsequent application to the design of adsorption treatment units, as well as for the evaluation of the fate of heavy metals in natural environments [5]. The removal of heavy metal ions from industrial wastewaters using different adsorbents is currently of great interest [2]. Studies so far have focused on adsorbents such as alumina, magnetite, pyrolusite, rutile, zirconia, hydrous manganese oxide, silica, geothite, heamatite, amorphous ferric oxide, bentonite, activated carbon, sphalerite, anatase, red mud, mica, illite, perlite and clay [6].

Kaolinite is the most abundant phyllosilicate mineral in highly weathered soils. It is a 1:1 aluminosilicate comprising a tetrahedral silica sheet bonded to an octahedral sheet through the sharing of oxygen atoms between silicon and aluminium atoms in adjacent sheets. Successive 1:1 layers are held together by hydrogen bonding of adjacent silica and alumina layers. The tetrahedral sheet carries a small permanent negative charge due to isomorphous substitution of Si^{4+} by Al^{3+}, leaving

* Corresponding author. Tel.: +90 266 612 10 00; fax: +90 266 612 12 15.
 E-mail addresses: malkan@balikesir.edu.tr (M. Alkan),
mdogan@balikesir.edu.tr (M. Doğan).

Nomenclature

C_0	initial dye concentration in aqueous solution (mol/L)
C_e	equilibrium copper ions concentration in solution (mol/L)
ΔH^0	heat of adsorption (kJ/mol)
K	adsorption constant
K_F	Freundlich constant
n	Freundlich isotherm exponent
q_e	equilibrium copper ions concentration on adsorbent (mol/g)
q_m	monolayer capacity of the adsorbent (mol/g)
R^2	regression coefficient
R_g	gas constant (J/K mol)
R_L	dimensionless separation factor
T	temperature (K)
V	volume of aqueous solution to be treated (L)
W	mass of adsorbent (g)

a single-negative charge for each substitution. Both the octahedral sheet and the crystal edges have a pH-dependent variable charge caused by protonation and deprotonation of surface hydroxyl (SOH) groups. Thus, two different populations of metal ion adsorption sites are present on the kaolinite surface. The intensive interaction between kaolinite and contaminants is primarily controlled by the surface acid–base properties [7]. A limited number of studies on the use of kaolinite as an adsorbent for copper removing from aqueous solutions have been found in the literature. At the same time, any one of these studies has not included the effect of acid-activation and thermal treatment of kaolinite samples. Suraj et al. investigated the adsorption of cadmium and copper by modified kaolinites and found that the modified amorphous derivative of kaolinite shows better adsorption of metal ions viz. Cd and Cu than the raw materials [8]; Bhattacharyya and Gupta the adsorption of chromium(VI) from water by clays (acid-activated kaolinite, poly(oxozirconium) kaolinite, and tetrabutylammonium kaolinite) and found that (i) clay minerals are capable of removing Cr(VI) from an aqueous solution; (ii) treatment of kaolinite with acid improved its adsorption capacity, but introduction of poly(oxozirconium) and tetrabutylammonium ions into kaolinite did not increase the capacity of kaolinite to take up more Cr(VI) ions [9]; Egirani et al. the copper and zinc removal from aqueous solution by mixed mineral systems [10]; Yavuz et al. the removal of copper, nickel, cobalt and manganese from aqueous solution by kaolinite, and found that the absorption affinity of kaolinite for metal ions is Cu(II) > Ni(II) > Co(II) > Mn(II) and sorption of copper, nickel, cobalt and manganese ions on kaolinite conformed to the linear form of Langmuir adsorption equation [11]; Gupta and Bhattacharyya, the adsorption of Ni(II) on clays [12]; and Wang et al., the use of kaolinite as a low-cost adsorbent for removing copper(II) ions from aqueous solutions as a function of pH, adsorbent concentration, ionic strength and solution temperature [13]. The aim of the present investigation was to study

Table 1
Some physicochemical properties of kaolinite

Color	White
Cation exchange capacity (meq/100 g)	13.00
Density (g/mL)	2.18
pH	7.90
Specific surface area (m²/g)	17
Hardness	2–3

the adsorption of copper ions onto kaolinite by measuring the effects of various parameters on the adsorption process such as pH, ionic strength, temperature, acid-activation and calcinations. Batch design was also drawn from experimental results.

2. Material and methods

2.1. Materials

The kaolinite sample was obtained from Güzelyurt (Aksaray, Turkey). All chemicals used in the study were obtained from Merck and Fluka, and were of analytical grade. The some physicochemical properties and chemical composition of kaolinite are given in Tables 1 and 2 [14]. The kaolinite sample was treated as follows [15] before being used in the experiments: the suspension containing 10 g/L kaolinite was mechanically stirred for 24 h; after about 2 min the supernatant suspension was filtered through a white-band filter paper. The solid sample was dried at 110 °C for 24 h, then sieved by a 100-mesh sieve. The particles under 100-mesh were used in further experiments. An infrared spectrophotometer, Perkin Elmer BX 1600 FTIR, was also used in order to confirm the identification of the constituents in raw and treated samples. IR spectroscopy is generally used in order to give information as far as the composition of a sample, its structure and its characteristic bonds are concerned. In addition, IR spectroscopy is applied on clay minerals in order to study the nature of isomorphic substitutions of cations in octahedral and tetrahedral sheet of the lattice [16] and the degree of crystallinity [17]. DTA/TG spectra of kaolinite were obtained by simultaneous DTA/TG (Perkin Elmer Diamond DTA/TG).

2.2. Acid- and heat activation

H_2SO_4 solutions were used to obtain the acid-activated kaolinite samples. The aqueous suspensions of kaolinite samples in

Table 2
Chemical composition of kaolinite

Constituent	Percentage present (%)
SiO_2	53.00
Al_2O_3	26.71
Na_2O	0.62
K_2O	1.39
CaO	0.57
Fe_2O_3	0.37
MgO	0.28
LoI	17.20

LoI: Loss of ignition.

0.2, 0.4 and 0.6 M H_2SO_4 solutions (so the acid/solid ratios were 1/5, 2/5, and 3/5 g/g) were refluxed with a reflux apparatus, filtered and washed with ultrapure water until no precipitation was observed upon the addition of $Ba_{(aq)}^{2+}$ into the filtrate, and finally dried at 110 °C for 24 h. Kaolinite samples calcinated have been prepared in the temperature range of 300–700 °C with a Nuve MF-140 furnace [18,19].

2.3. Method

Aqueous solutions of copper were prepared from copper nitrate. Ultrapure water was used throughout the study. The adsorption experiments were carried out by mechanically shaking 0.5 g of the kaolinite samples with 50 mL of aqueous solution containing the metal ions in a concentration range of 1.575×10^{-5}–1.575×10^{-3} mol/L for the required pH (natural~4.5), temperature (25 °C) and ionic strength (1×10^{-3} mol/L) in 100 mL covered polyethylene containers. The equilibration time was found to be 16 h but for practical reasons the adsorption experiments were run for 24 h. Polyethylene flasks were shaken (180 rpm) at constant temperature using a GFL model incubator orbital shaker with temperature control in the range of 4–60 °C. The solution pH was controlled by addition of HCl and NaOH by using an Orion 920A pH meter with a combined pH electrode. The pH meter was standardized with NBS buffers before every measurement. At the end of the equilibration period, the kaolinite was separated by filtration. The concentration of copper ions was determined by using a Unicam 929 Atomic Absorption Spectrometer with air–acetylene flame. Quantification of the metals was based upon calibration curves of standard solutions of copper ion. These calibration curves were determined several times during the period of analysis. All the adsorption studies were repeated twice; hence, the reported value of metal ion adsorbed is the average of two measurements. Blanks containing no Cu^{2+} were used for each series of experiments. The adsorption capacity of the kaolinite was evaluated using the following expression:

$$q_e = (C_0 - C_e)\frac{V}{W} \tag{1}$$

where q_e is the amount of metal ion adsorbed onto the unit mass of the kaolinite (mol/g); C_0 and C_e, the concentration of the metal ion in the initial solution and in the aqueous phase after treatment for a certain period of time (mol/L); V, the volume of the aqueous phase (L); and W, the amount of kaolinite used (g) [6].

3. Results and discussion

3.1. Adsorption isotherm

The isotherm plot for copper adsorption on kaolinite with a fixed adsorbent dose of 10 g/L at a pH of natural~4.5 ± 0.1 at constant ionic strength (1×10^{-3} mol/L) is shown in Fig. 1. The shape of the isotherms is characteristic of Langmuir-type adsorption behavior. It is clear from the figure that as the concentration of the ions increased, adsorption increased first rapidly, then
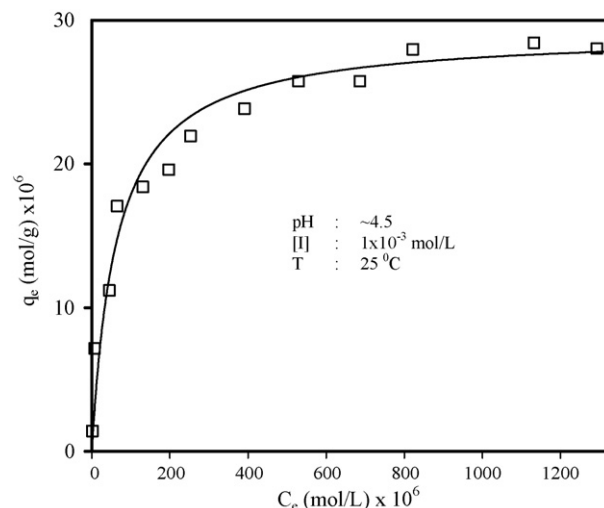

Fig. 1. The plot of adsorption isotherm.

slowed down, and adsorption saturation values were reached. The copper adsorption is higher for greater values of initial copper concentration. This occurs because of the more efficient utilization of the adsorptive capacities of the adsorbent owing to a greater driving force [4].

3.2. Adsorption parameters

3.2.1. Effect of pH

Because of the protonation and deprotonation of the acidic and basic groups of the adsorbents, its adsorption behavior for metal ions is influenced by the pH value, which affects the surface structure of sorbents, the formation of metal hydroxides, and the interaction between sorbents and metal ions [20]. Therefore, the pH dependence of adsorption for metal ions was investigated in detail. The adsorption of copper on kaolinite was studied in the initial pH range 3–6 for a fixed absorbent dose of 10 g/L at a constant ionic strength (1×10^{-3} mol/L) (Fig. 2). This figure shows that the adsorption behavior of metal ions is
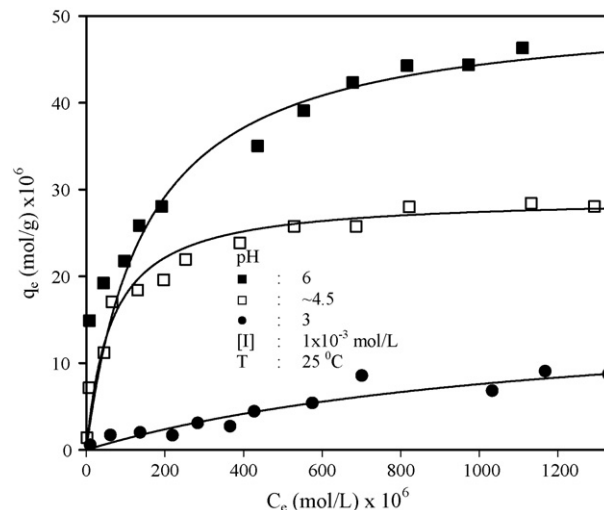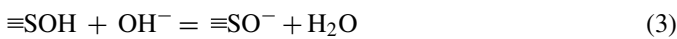

Fig. 2. Effect of initial pH on adsorption of copper(II) ions onto kaolinite.

more sensitive to pH changes. It is obvious that the higher the initial pH value the larger the adsorption capacity. A general increase in copper adsorption with increasing pH of the solution has been observed up to pH 6.0. The increase in the metal removal as the pH increases (i.e., as the solution becomes more basic) can be explained on the basis of a decrease in competition between proton and metal species for the surface sites, and by the decrease in positive surface charge, which results in a lower columbic repulsion of the sorbing metal [5]. The surface charge of adsorbents is usually characterised by a point of zero charge or pH_{zpc}. The surface charge of a adsorbent is positive at $pH < pH_{zpc}$ and it is negative for $pH > pH_{zpc}$. We previously found that kaolinite had a pH_{zpc} at pH 2.35 [14]. The surface is positive at lower pH than pH_{zpc} where reaction (2) predominates, and is negative at higher pH than pH_{zpc} when reaction (3) takes over:

$$\equiv SOH + H^+ = \equiv SOH_2^+ \tag{2}$$

$$\equiv SOH + OH^- = \equiv SO^- + H_2O \tag{3}$$

At $pH = pH_{zpc}$

$$[\equiv SO^-] = [\equiv SOH_2^+] \tag{4}$$

At pH values higher than pH_{zpc}, the association of copper cations with more negatively charged kaolinite surface because of increasing $\equiv SO^-$ groups can more easily take place. As the pH increases from 3.0 to 6.0, the ion exchange sites become increasingly ionized. High removal efficiency at $pH > pH_{zpc}$ can therefore be attributed to electrostatic interactions between the positively charged copper(II) ions and negatively charged binding sites on kaolinite surface. Similarly, poor removal efficiency at $pH < pH_{zpc}$ indicates that the kaolinite surface bears a net positive charge which would impede the approach of the positively charged copper(II) ions. In addition, at low pH values an excess of protons can compete effectively with the copper(II) ions for binding sites on kaolinite surface [21]. The pH-removal curves are shifted to more alkaline regions. This effect has been attributed to the surface binding of low-affinity surface sites as high-affinity ones begin to reach saturation, leading to a reduction in the removal efficiency [5].

3.2.2. Effect of ionic strength

It is known that salts have a significant effect on the adsorption process. In this work, sodium chloride (NaCl) was selected as model salt to investigate its influence on the sorption of copper ions by kaolinite. The kaolinite was exposed to series of solutions containing mentioned salt in the concentration range of 0.0001–0.1 mol/L. In order to investigate the effect of ionic strengths on the adsorption of copper ions, sodium chloride was added into the suspensions. The results are shown in Fig. 3 which reveals that adsorption decreases with increasing concentration of sodium chloride. Since the presence of NaCl in the solution screens the electrostatic interaction of opposite charges of the kaolinite surface and the metal ions, the adsorbed amount should decrease with increase of NaCl concentration [22].
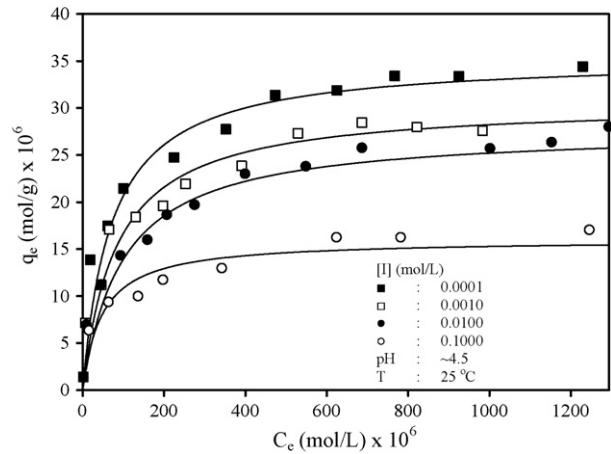

Fig. 3. Effect of ionic strength on adsorption of copper(II) ions onto kaolinite.

3.2.3. Effect of temperature

The effect of temperature on adsorption is important not only because it affects the rate and extent of adsorption but also due to the fact that temperature dependence of adsorption provides information about possible adsorbate-adsorbent interaction [23]. In the temperature range of 25–55 °C, the adsorption capacity of kaolinite for the copper ion was determined. The results of the studies on the influence of temperature on cation adsorption are presented in Fig. 4 in terms of amount of metal removed versus temperature. It can be seen that temperature has only an important effect on adsorption thus confirming the predictions of the enthalpy calculations. The results indicate that the adsorption removal increased with increase of the solution temperature. This shows that the adsorption process is an endothermic process.

3.2.4. Effect of acid-activation

The effects of acid-activation on the adsorption of copper ions on kaolinite are given in Fig. 5. The adsorbed amounts of copper ions decreased with the increasing concentration of H_2SO_4 used for the acid-activation. This may be due to the partial destruction of kaolinite structure, as was shown by Gonzàlez-Pradas
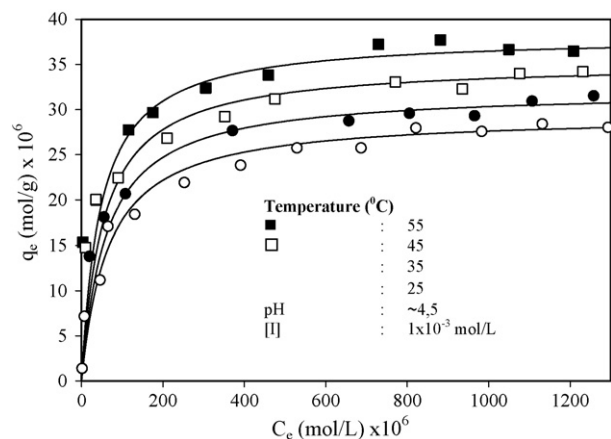

Fig. 4. Effect of solution temperature on adsorption of copper(II) ions onto kaolinite.
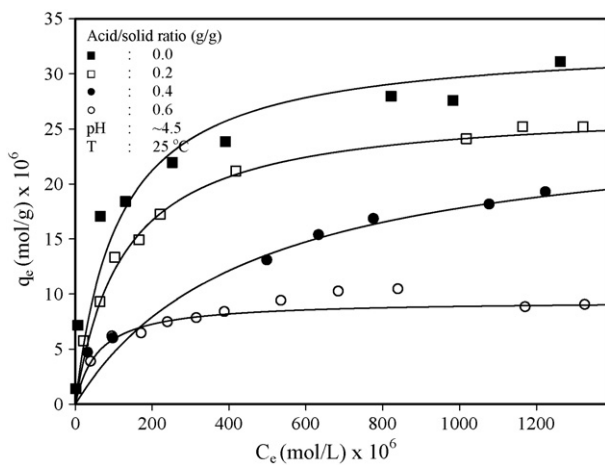
Fig. 5. Effect of acid-activation on adsorption of copper(II) ions onto kaolinite.

et al. [24] and López-Gonzàlez and Gonzàlez-Garcìa [25] for bentonite, and also may be due to the specific adsorption of H+ ions on the kaolinite surface.

3.2.5. Effect of calcination temperature

Fig. 6 has shown the adsorption of copper ions onto calcinated and natural kaolinite samples. As can be seen in this figure, the amount adsorbed of copper ions on kaolinite has decreased with increasing activation temperature. Fig. 7 presents the IR spectra of natural and calcinated kaolinite samples. Assignment of the FTIR vibrational frequencies of the experimental and literature data of kaolinite are given in Table 3 [26–30]. The main IR functional bands of the kaolinite given in Fig. 7 should be compared to the literature values. The peak at $3621\,cm^{-1}$ has been assigned to inner-hydroxyl group, the $3696\,cm^{-1}$ corresponds to the inner-surface O–H group, the peak at 795 assign to ν_s(Si–O–Si) and finally, 469 and $429\,cm^{-1}$ peaks are adapted to the deformation vibration of Si–O. FTIR spectra of calcinated kaolinite at $600\,^{\circ}C$ are also shown in Fig. 7 and the vibration bands for metakaolinite are given in Table 4 [26,31,32]. The broad bands of metakaolinite, located at 795 and $800\,cm^{-1}$ assigned to the Al–O bonds in Al_2O_3 is observed. The vibration
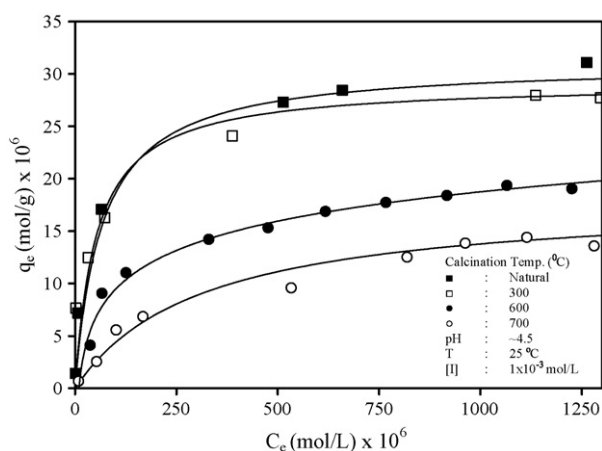

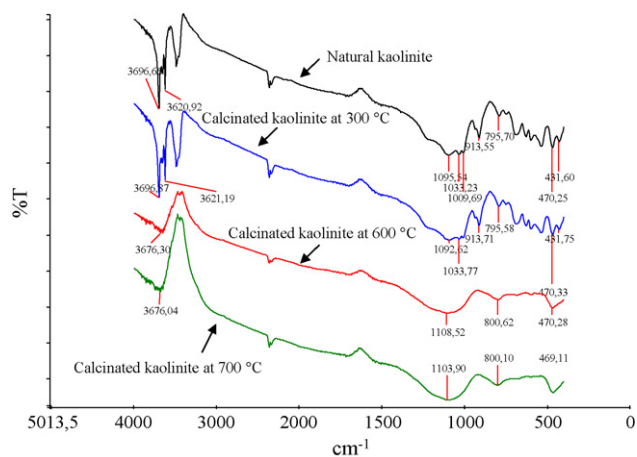Fig. 6. Effect of calcination temperature on adsorption of copper(II) ions onto kaolinite.

Fig. 7. FTIR spectra of natural and calcinated kaolinite samples.

Table 3
IR vibrational frequencies of the experimental and literature data of kaolinite [26–30]

Vibrations	Wavenumber (cm^{-1}) (experimental)	Literature wave number (cm^{-1})
ν(OH)	3621, 3622	3620
ν(OH)	3696	3695
δ(OH)	913	912
ν(OH)	1092, 1095, 1103, 1108	1116, 1010
Si–O deformation	469, 470, 431	469, 428
ν_s(Si–O–Si)	795	794, 754

band at $1108\,cm^{-1}$ for metakaolinite assigned to the stretching Si–O bonds in SiO_2 [30]. These bands proved the conversion of kaolinite to metakaolinite phase, which was obtained from the calcinated kaolinite at $600\,^{\circ}C$. Simultaneous DTA/TG can differentiate between peaks associated with mass loss and those associated with phase transition. DTA has been used very widely in the study of thermal reactions of clay minerals. These reactions include dehydration of adsorbed water, dehydroxylation (evolution of water from hydroxyls belonging to the clay skeleton) followed by the transformation of the clay to a meta-phase and recrystallization of the meta-phase into a crystalline phase [33,34]. The DTA peak temperatures are characteristic for each mineral and DTA curves are applicable for the identification and determination of many clays [35,36]. The DTA and d(DTA) curves of the kaolinite (Fig. 8) show strong endothermic peak at $560\,^{\circ}C$ due to dehydroxylation and at about $1030\,^{\circ}C$ due to the formation of new solid phase. As seen from TG and d(TG) curves in Fig. 9, dehydroxylation of kaolinite results in a mass

Table 4
Vibration bands of metakaolinite [26,31,32]

Vibrations	Wave number (cm^{-1}) (experimental)	Literature wave number (cm^{-1})
Al–O bonds	795, 800	800
ν(SiO)	1108	1090
O–Si–O deformation	469, 470	467

Fig. 8. DTA and d(DTA) spectrums of kaolinite under nitrogen atmosphere.

loss of 11.345%. In the first step of transformation, kaolinite was transformed to metakaolinite phase with loss of structural hydroxyl groups during the occurrence of an endotherm. In the second step, metakaolinite decomposes and forms spinel phase generally during heating around the first exothermic peak temperature. When the kaolinite is heated, the adsorbed water is liberated at above 100 °C and the weakest part of the chemical bond is broken or perturbed; then dehydroxylation takes place at 400–600 °C range. The main changes pointed out by DTA/TGA, during the heating of the samples are indicated as follows [17,30]: (i) $T < 100$ °C: low temperature release of the absorbed water in pores, on the surfaces, etc.; (ii) 100–400 °C: mass loss that can be correlated with a pre-dehydration process, which takes place as a result of the reorganization in the octahedral layer, first occurring at the OH of the surface; (iii) 400–650 °C: dehydroxylation of kaolinite and formation of

metakaolinite according to the following reaction:

$$Al_2Si_2O_5(OH)_4(s) \rightarrow Al_2Si_2O_5(OH)_xO_{2-x}(s)$$
$$+ (2-x/2)H_2O(l) \qquad (5)$$

with a low value of x (about 10% of residual hydroxyl groups in metakaolinite); (iv) 950 °C: decomposition of metakaolinite was observed according to the following chemical reaction:

$$2\underset{\text{(metakaolinite)}}{(2SiO_2 \cdot Al_2O_3))(s)} \overset{950\,°C}{\rightarrow} \underset{\text{(Al–Si–spinel)}}{Si_3Al_4O_{12}(s)} + \underset{\text{(amorphous)}}{SiO_2(s)} \qquad (6)$$

The kaolinite structure consists of a single silica tetrahedral sheet and a single alumina octahedral sheet combined to form the kaolinite unit layer. These unit layers are stacked one over the other. During calcination, the silicon atoms experience a range of environments of differing distortion due to dehydroxylation.

Fig. 9. TG and d(TG) spectrums of kaolinite under nitrogen atmosphere.

The aluminium atoms mostly transform from octahedral to tetrahedral geometry. As the calcination temperature increases, the structure becomes more distorted, and finally amorphous silica is liberated [37]. For kaolinite, dehydroxylation might result in the disturbance of the $Al(O,OH)_6$ octahedral sheet by the outer hydroxyls, but does not much effect on the SiO_4 tetrahedral sheet due to the more stable inner-hydroxyl groups. The outer hydroxyls of octahedral sheets may be more easily removed by heating than inner ones that will maintain a more ordered SiO_4 tetrahedral group in structure during dehydroxylation. After heating at 950 °C, the SiO_4 groups combine with AlO_6 group to form the Al–Si spinel phase that in a short range order structure [17,30]. After the thermal treatment of sample, the transformation of kaolinite to metakaolinite is confirmed by the absence of detectable Al–O–H bands at 913 cm^{-1}. The reduction of band at 539 and 913 cm^{-1} and the appearance of a new band at 800 cm^{-1} can be connected with the change from octahedral coordination of Al^{3+} in kaolinite to tetrahedral coordination in metakaolinite. The bands at 1095 cm^{-1} are assigned to amorphous SiO. Si–O coordination bands at 1033 cm^{-1} are observed as a result of the Si–O vibration. The band at 1033 cm^{-1} represents the stretching of Si–O in the Si–O–Si groups. The band at 471 cm^{-1} is due to Si–O–Al (octahedral) and Si–O–Si bending vibrations for kaolinite [17]. The intensity of hydroxyl peaks has decreased with increase in calcination temperature, as seen from Fig. 7. Therefore, the decrease in the amount adsorbed of copper ions with increasing activation temperature may be a result of the removal of most of the micropores due to heating the sample [19] and due to the decrease in OH groups in kaolinite during the calcination process, as can be seen from Fig. 7.

3.3. Adsorption models

An adsorption isotherm is used to characterize the interaction of each heavy-metal ion with the adsorbent. This provides a relationship between the concentration of heavy-metal ion in the solution and the amount of heavy-metal ion adsorbed onto the solid phase when the two phases were at equilibrium [20]. The adsorption data obtained for equilibrium conditions have been analyzed by using the following linear forms of the Freundlich and Langmuir isotherms

3.3.1. Langmuir isotherm

The Langmuir adsorption model assumes that molecules are adsorbed at a fixed number of well-defined sites, each of which can only hold one molecule and no transmigration of adsorbate in the plane of the surface. These sites are also assumed to be energetically equivalent and distant to each other so that there are no interactions between molecules adsorbed to adjacent sites. The linear form of the Langmuir isotherm is represented by the following equation [4,20]:

$$\frac{C_e}{q_e} = \frac{1}{q_m K} + \frac{C_e}{q_m} \tag{7}$$

where q_e is the amount adsorbed (mol/g), C_e is the equilibrium concentration of the adsorbate ions (mol/L), and q_m and K are Langmuir constants related to maximum adsorption capacity

(monolayer capacity) (mol/g) and energy of adsorption (L/g), respectively. When C_e/q_e is plotted against C_e, a straight line with slope $1/q_m K$ and intercept $1/q_m$ is obtained, which shows that the adsorption of metal ions follows Langmuir isotherm model. Langmuir parameters, q_m and K, were calculated from the slope and intercept of the graphs and were given in Table 5.

3.3.2. Freundlich isotherm

Freundlich isotherm is an empirical equation that encompasses the heterogeneity of sites and the exponential distribution of sites and their energies [38]. The adsorption data for copper ions on kaolinite have also been analysed using the logarithmic form of the Freundlich isotherm as shown below [4]:

$$\ln q_e = \ln K_F + \frac{1}{n} \ln C_e \tag{8}$$

where K_F and n are Freundlich constants related to adsorption capacity and adsorption intensity, respectively. When $\ln q_e$ is plotted against $\ln C_e$, a straight line with slope n and intercept K_F is obtained. The intercept of the line, K_F, is roughly an indicator of the adsorption capacity and the slope, n, is an indication of adsorption intensity. The values obtained for the Freundlich variables for the adsorption of copper ions are given in Table 5. The n values, $n > 1$, dictate favorable adsorption [39].

Adsorption isotherms were obtained in terms of Eqs. (7) and (8) by using experimental adsorption results in these equations. Table 5 has shown the results of Langmuir and Freundlich isotherm analyses calculated for adsorption of copper ions on kaolinite from aqueous solutions at different pH, ionic strength, temperatures, acid-activations and calcinations. The isotherm data were calculated from the least square method and the related correlation coefficients (R^2-values) are given in Table 5. As seen from Table 5, the Langmuir equation represents the adsorption process very well; the R^2 values were all higher than 0.99, indicating a very good mathematical fit. The fact that the Langmuir isotherm fits the experimental data very well may be due to homogenous distribution of active sites on kaolinite surface; since the Langmuir equation assumes that the surface is homogenous. The applicability of the Langmuir isotherm in the present system indicates the monolayer coverage of copper ions on the outer surface of the adsorbent [40].

Further, the essential characteristics of the Langmuir isotherm are defined by a dimensionless separation factor, R_L, which is defined by the following relationship [22]:

$$R_L = \frac{1}{1 + KC_e} \tag{9}$$

The value of R_L indicates the type of the isotherm to be either unfavorable ($R_L > 1$), linear ($R_L = 1$), favorable ($0 < R_L < 1$) or irreversible ($R_L = 0$). The values of R_L reported in Table 5 have been found to be between 0 and 1, indicating favorable adsorption for copper ions on kaolinite for the entire concentration range studied.

A comparison between the adsorption capacities of kaolinite and other adsorbents under similar conditions is presented in Table 6 [9,21,41,42]. When comparing our results for kaolinite with the results of others, it can be concluded that the kaolinite

Table 5
Isotherm constants for copper adsorption on kaolinite

Parameter					Freundlich isotherm			Langmuir isotherm			
Temperature (°C)	pH	[I] (mol/L)	Calcination temperature (C°)	Acid/solid ratio (g/g)	n	$K_F \times 10^{-4}$	R^2	q_m (mol/g) $\times 10^6$	K (L/mol) $\times 10^{-4}$	R^2	R_L
25	~4.5	0.0010	–	–	3.50	2.13	0.9778	29.41	153	0.9965	0.98–0.05
35	~4.5	0.0010	–	–	4.90	1.28	0.9737	32.15	166	0.9970	0.75–0.04
45	~4.5	0.0010	–	–	5.40	1.26	0.9866	35.21	187	0.9963	0.84–0.04
55	~4.5	0.0010	–	–	6.50	1.08	0.9876	38.17	234	0.9972	0.92–0.03
25	~4.5	0.1000	–	–	4.80	6.42	0.9735	14.32	25	0.9976	0.72–0.03
25	~4.5	0.0100	–	–	3.61	1.80	0.9890	28.49	135	0.9943	0.97–0.05
25	~4.5	0.0001	–	–	4.34	1.67	0.9901	35.33	141	0.9925	0.78–0.05
25	3	0.0010	–	–	1.80	3.30	0.9857	16.78	8.24	0.9973	0.95–0.98
25	6	0.0010	–	–	4.19	2.17	0.9638	29.54	158	0.9911	0.99–0.98
25	~4.5	0.0010	–	0.2	3.20	2.70	0.9644	27.10	80	0.9949	0.37–0.20
25	~4.5	0.0010	–	0.4	2.17	4.17	0.9919	25.90	22	0.9920	0.93–0.33
25	~4.5	0.0010	–	0.6	3.03	1.12	0.9950	9.40	17	0.9995	0.6–0.04
25	~4.5	0.0010	300	–	4.73	1.17	0.9779	29.15	189	0.9964	0.95–0.04
25	~4.5	0.0010	600	–	2.95	1.17	0.9957	20.70	90	0.9921	0.75–0.08
25	~4.5	0.0010	700	–	1.61	10.00	0.9495	18.08	32	0.9944	0.77–0.19

Table 6
Comparison with other adsorbents

Adsorbents	Metal ions	q_m (mol/g) $\times 10^5$	References
Unexpanded perlite	Copper	0.417	[9]
Expanded perlite	Copper	0.28	[9]
Sepiolite	Copper	60.60	[41]
Activated carbon	Copper	7.00	[21]
Rice hulls	Copper	6.14	[42]
Kaolinite	Copper	2.94	In this study

adsorbed metal ions as effectively as the other adsorbents listed. A lower kaolinite production cost compared to other adsorbents such as activated carbon is another advantage of kaolinite for use as an adsorbent.

3.4. Heat of adsorption

The heat of adsorption of a given adsorption process is one of the most useful parameters in surface science studies. The isosteric heat of adsorption, ΔH^0, from the adsorption data at various temperatures as a function of coverage fraction ($\theta = q_e/q_m$) can be estimated from the following equation [43]:

$$\frac{\Delta H^0}{R_g} = \left[\frac{\partial(\ln C_e)}{\partial(1/T)} \right]_{\theta=0.5} \tag{10}$$

where R_g is the gas constant. Fig. 10 shows the plots of $-\ln C_e$ against $1/T$. The value of ΔH^0 was calculated at a specific coverage fraction of 0.5 as 16.65 kJ/mol. The value of adsorption heat shows that physical adsorption takes place in the adsorption of copper(II) ion on kaolinite. Since adsorption is an endothermic process, it would be expected that an increase in solution temperature would result in an increase in adsorption capacity [22]. Similar result was also found for the adsorption of copper on perlite [6].

3.5. Single stage batch adsorption

Adsorption isotherms can be used to predict the design of single stage batch adsorption systems [44]. The schematic diagram
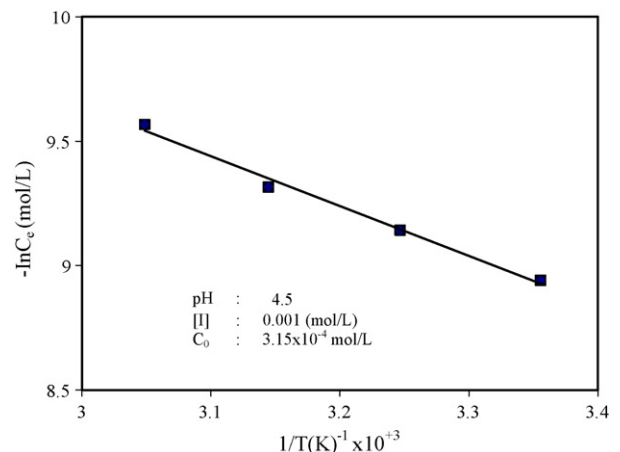

pH : 4.5
[I] : 0.001 (mol/L)
C₀ : 3.15x10⁻⁴ mol/L

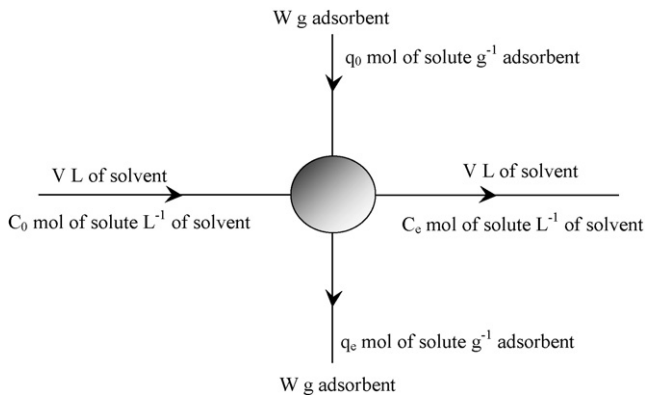Fig. 10. The plot of $-\ln C_e$ vs. $1/T$.

Fig. 11. A single-stage batch adsorber.

for a single stage adsorption process is shown in Fig. 11. The solution to be treated contains V L of water, and the metal concentration is reduced from C_0 to C_e in the adsorption process. In the treatment stage, W g adsorbent is added and the metal concentration on kaolinite changes from $q_0 = 0$ to q_e. The mass balance that equates the metal removed from the liquid effluent to the that accumulated by kaolinite is

$$V(C_o - C_e) = W(q_e - q_0) = Wq_e \qquad (11)$$

In the case of the adsorption of copper ion on kaolinite, the Langmuir isotherm gives the best fit to experimental data. The Langmuir data may now be applied to Eq. (11) and substituting for q_e from Eq. (7) and rearranging gives

$$\frac{W}{V} = \frac{C_0 - C_e}{q_e} \equiv \frac{C_0 - C_e}{(q_m KC_e / 1 + KC_e)} \qquad (12)$$

Eq. (12) permites analytical calculation of the adsorbent solution ratio for a given change in solution concentration, C_0 to C_e. Fig. 12 shows a series of plots derived from Eq. (12) for the adsorption of copper ions on kaolinite. An initial copper concentration of 7.86×10^{-4} mol/L is assumed and the figure shows the amount of effluent which can be treated to reduce the cop-
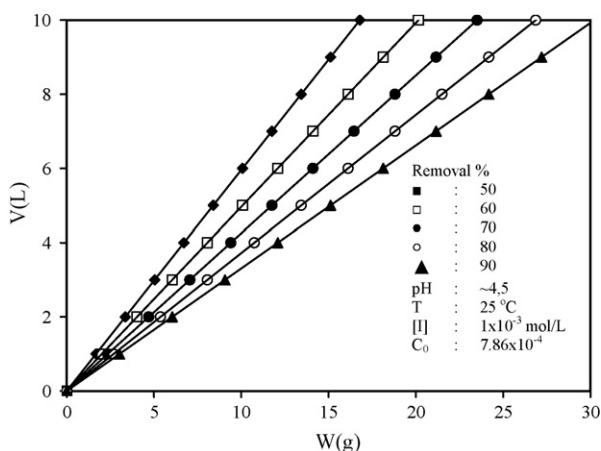
Fig. 12. Volume of effluent (V) treated against adsorbent mass (W) for different percentage copper removal.

per content by 90, 80, 70, 60 and 50% using various masses of kaolinite.

3.6. Conclusion

The results of present investigation show that kaolinite, low cost materials, has suitable adsorption capacity with regard to the removal of copper ions from its aqueous solutions. The adsorbed amount of copper ions decreased with increase in ionic strength, acid-activation and calcination temperature, but the adsorbed amount of copper ions increased with increase in pH and temperature. The experimental equilibrium data obtained were applied to the Langmuir and Freundlich isotherm equations to test the fitness of these equations. The experimental data were correlated reasonably well by the Langmuir adsorption isotherm and the isotherm parameters (q_m and K) have been calculated. The enthalpy change for the adsorption process was indicative of the endothermic nature of adsorption and a physical adsorption. The dimensionless separation factor (R) showed that kaolinite can be used for removal of copper ions from aqueous solutions. The results of this research were compared to the published data in the same field, and found to be in agreement with most of them. The batch design may be useful for environmental technologist in designing treatment plants for metal removal from wastewaters.

References

[1] Z. Aksu, Ü. Acikel, T. Kutsal, J. Chem. Technol. Biotechnol. 70 (1997) 368–378.
[2] S. Kocaoba, T. Akyuz, Desalination 181 (2005) 313–318.
[3] V.J. Inglezakis, M.D. Lozidou, H.P. Grigoropoulou, Water Res. 36 (2002) 2784–2792.
[4] C.K. Jain, I. Ali, Hydrol. Process 14 (2000) 261–270.
[5] A. Seco, P. Marzal, C. Gabaldon, J. Chem. Technol. Biotechnol. 68 (1997) 23–30.
[6] M. Alkan, M. Doğan, J. Colloid Interface Sci. 243 (2001) 280–291.
[7] D.G. Schulze, in: J.B. Dixon, S.B. Weed (Eds.), Minerals in Soil Environment, second ed., Soil Science Society of America, Madison, 1989, p. 1.
[8] G. Suraj, C.S.P. Iyer, M. Lalithambika, Appl. Clay Sci. 13 (1998) 293–306.
[9] K.G. Bhattacharyya, S.S. Gupta, Ind. Eng. Chem. Res. 45 (2006) 7232–7240.
[10] D.E. Egirani, A.R. Baker, J.E. Andrews, J. Colloid Interface Sci. 291 (2005) 319–325.
[11] O. Yavuz, Y. Altunkaynak, F. Güzel, Water Res. 37 (2003) 948–952.
[12] S.S. Gupta, K.G. Bhattacharyya, J. Colloid Interface Sci. 295 (2006) 21–32.
[13] X.S. Wang, J. Wang, C. Sun, Adsorpt. Sci. Technol. 24 (6) (2006) 517–530.
[14] M. Alkan, Ö. Demirbaş, M. Doğan, Micropor. Mesopor. Mater. 83 (2005) 51–59.
[15] M. Doğan, M. Alkan, J. Colloid Interface Sci. 267 (2003) 32–41.
[16] V. Stubican, R. Rustum, Am. Mineral. 46 (1961) 32–51.
[17] G. Kakali, T. Perraki, S. Tsivilis, E. Badogiannis, Appl. Clay Sci. 20 (2001) 73–80.
[18] M. Doğan, M. Alkan, Y. Onganer, Water Air Soil Pollut. 120 (2000) 229–248.
[19] M. Alkan, S. Celikcapa, O. Demirbas, M. Doğan, Dyes Pigments 65 (2005) 251–259.
[20] P.E. Duru, S. Bektas, O. Genc, S. Patir, A. Denizli, J. Appl. Polym. Sci. 81 (2001) 197–205.
[21] K.H. Chu, M.A. Hashim, J. Chem. Technol. Biotechnol. 75 (2000) 1054–1060.

[22] Y. Ozdemir, M. Doğan, M. Alkan, Micropor. Mesopor. Mater. 96 (2006) 419–427.

[23] A.K. Bajpai, N. Vishwakarma, Colloids and Surf. A: Physicochem. Eng. Aspects 220 (2003) 117–130.

[24] E. Gonzàlez-Pradas, M. Villafranca-Sànchez, A. Valverde-Garcìa, M. Socias-Viciana, J. Chem. Technol. Biotechnol. 42 (1998) 105.

[25] J.D. López-Gonzàlez, S. Gonzàlez-Garcìa, An. Fis. Quim. 50-B (1954) 465.

[26] S. Markovic, V. Dondur, R. Dimitrijevic, J. Mol. Struct. 654 (2003) 223–234.

[27] C.T. Johnston, D.L. Bish, J. Eckert, L.A. Brown, J. Phys. Chem. B 104 (2000) 8080–8088.

[28] S. Yariv, I. Lapides, J. Therm. Anal. Calorim. 56 (1999) 865–884.

[29] N.J. Saikia, D.J. Bharali, P. Sengupta, D. Bordoloi, R.L. Goswamee, P.C. Saikia, P.C. Bothakur, Appl. Clay Sci. 24 (2003) 93–103.

[30] M. Alkan, C. Hopa, Z. Yilmaz, H. Güler, Microporous Mesoporous Mater. 86 (2005) 176–184.

[31] A. Demortier, N. Gobeltz, J.P. Lelieur, C. Duhayon, Int. J. Inorg. Mater. 1 (1999) 129–134 .

[32] E.M. Flaningen, H.A. Khatami, H.A. Szymanski, Molecular Sieve Zeolites 16 (1971) 201.

[33] W. Smykatz-Kloss, Differntial Thermal Analysis. Application and Results in Mineralogy, Springer, Berlin, 1974.

[34] A. Langier-Kuzniarowa, Thermochim. Acta 148 (1989) 413–420.

[35] R.C. Mackenzie, The Differential Thermal Investigation of Clays; Mineralogical Society, Clay Minerals Group, London, 1957.

[36] R.C. Mackenzie, Simple Phyllosilicates Based on Gibbsite and Brucite-like Sheets. Differential Thermal Analysis, 1, Academic Press, London, 1970, pp. 497–537.

[37] S. Chandrasekhar, P.N. Pramada, J. Porous Mater. 6 (1997) 283–297.

[38] N.K. Lazaridis, D.D. Asouhidou, Water Res. 37 (2003) 2875–2882.

[39] G. Atun, G. Hisarli, Chem. Eng. J. 95 (2003) 241–249.

[40] E. Rubin, P. Rodriguez, R. Herrero, J. Cremades, I. Barbara, M.E. Sastre de Vicente, J. Chem. Technol. Biotechnol. 80 (2005) 291–298.

[41] A. Türkyilmaz, Electrokinetic properties of sepiolite and copper adsorption. MSc. Thesis. Balikesir University, 2005, Balikesir, Turkey (Turkish).

[42] M. Teker, M. İmamoglu, Ö. Saltabaş, Turk. J. Chem. 23 (1999) 185–191.

[43] E. Gonzalez-Pradas, M. Villafranca-Sanchez, M. Socias-Viciana, J. Chem. Technol. Biotechnol. 39 (1987) 19.

[44] G. McKay, M.S. Otterburn, A.J. Aga, Water Air Soil Pollut. 24 (1985) 307.